Applied Surface Science 456 (2018) 342–350

Contents lists available at ScienceDirect

Applied Surface Science

journal homepage: www.elsevier.com/locate/apsusc

Full Length Article

Laser processing of silicon for photovoltaics and structural phase transformation

Zeming Sun, Mool C. Gupta*

Charles L. Brown Department of Electrical and Computer Engineering, University of Virginia, Charlottesville, VA 22904, United States

ARTICLE INFO

Keywords:
Phase transformation
Laser processing
Transmission electron microscopy (TEM)
Raman spectroscopy
Silicon
Photovoltaics

ABSTRACT

High-power nanosecond-pulse-width laser processing is attracting increasing attention for the manufacturing of low-cost high-performance silicon photovoltaic and microelectronic devices. However, the lack of fundamental understanding of laser induced defect formation and phase transformation hinders the broader application of lasers. To address this, we systematically investigated the laser-induced phase transformation using different laser systems of 532 nm wavelength, 1.3 ns pulse width and 1064 nm wavelength, 50 ns pulse width. In doing this, we carried out cross-sectional transmission electron microscopy (TEM) and Raman spectroscopy line-mapping studies to analyze the local phase information across the laser processed spot. We demonstrate the retention of single-crystalline phase under 1.64 J/cm^2 fluence using a 532 nm wavelength laser. This retention of single-crystalline phase is important for ensuring high effective carrier lifetime and hence high photovoltaic conversion efficiency. Moreover, the 1064 nm wavelength laser processed samples under increasing fluences showed a phase evolution from crystalline to amorphous/polycrystalline transformation. After 1064 nm laser processing above 1.47 J/cm^2 fluences, microtwins with dislocations were observed, in addition to increasing expansion stress. Additionally, the appearance of extra spots in the (3 1 1) diffraction ring pattern obtained by TEM studies of samples processed at 1.60 J/cm^2 fluence using a 1064 nm laser, demonstrates the generation of a high density of dislocations.

1. Introduction

Recently, high-power laser processing has attracted considerable attention in the silicon photovoltaic industry in order to achieve the goal of high-efficiency low-cost devices [1]. The major reason is that laser processing provides a potential route for replacing the high-temperature techniques, high-vacuum processes, and complex lithographic steps required for traditional photovoltaic fabrication. A variety of effort has been spent on laser ablation [2–7], laser microtexturing [4,5], laser edge isolation [6,7], laser doping [8–10], laser transferred metal contacts [11], laser firing contacts [12], laser annealing [13–15], laser oxidation for surface passivation [16,17], and laser cutting [18]. The wide use of lasers in photovoltaics has led to a renaissance of investigation into nanosecond-pulse-width laser processed silicon.

The current challenge for laser-based Si-photovoltaic applications is a non-equilibrium phase change due to ultra-rapid melting and re-solidification during laser processing. The generation of disordered amorphous and polycrystalline phases can be extremely detrimental to the silicon's electrical properties and the device's performance [13–15,19–21]. Hence, a fundamental understanding of the origin of phase transformation during laser processing of silicon is required.

To date, ion-induced phase transformation in silicon have been well studied [22,23]. Existing investigations into laser-induced phase transformation merely focus on amorphous-to-crystalline changes and their laser annealing applications [24–26]. However, literature on crystalline-to-amorphous/polycrystalline transformation after laser processing is very limited and only several papers report results using ultrafast lasers only [27–29] or using simulations [30]. To the authors' knowledge, no comprehensive study on Si phase transformation under nanosecond-pulse-width laser processing was found. Crystalline-to-amorphous/polycrystalline phase changes are of particular interest since precise control of initial phase is essential for broader applications of nanosecond-pulse-width lasers in the Si photovoltaic and electronic industry. The lack of detailed fundamental studies in the experimental regime of laser-induced phase changes of Si is the major motivation for this work. A systematic experimental investigation was carried out to understand the mechanisms of phase changes during laser processing. More importantly, it is essential to identify the necessary laser parameters to avoid phase transformation in order to achieve superior device performance.

---

* Corresponding author.
E-mail address: mgupta@virginia.edu (M.C. Gupta).

https://doi.org/10.1016/j.apsusc.2018.06.092
Received 13 March 2018; Received in revised form 8 June 2018; Accepted 11 June 2018

In this work, we evaluate laser induced phase transformation using different laser systems of 532 nm wavelength, 1.3 ns pulse width and 1064 nm wavelength, 50 ns pulse width. Moreover, we correlate cross-sectional TEM images and Raman line-map spectra to identify local phase changes at different positions within the laser processed spot. We demonstrate the retention of a single crystalline phase after 532 nm laser processing via control of laser fluence, which is beneficial to achieving high photovoltaic conversion efficiency. Furthermore, we present and explain the phase evolution relationship with varied 1064 nm laser processing fluences. Besides phase information, we also present microstructural and stress information determined from high-magnification TEM images and quantification of diffraction indices.

2. Experimental

2.1. Silicon wafer

Single-side polished n-type (phosphorous-doped) FZ c-Si wafers were used, with a thickness of 200 μm, orientation of ⟨1 0 0⟩, and resistivity of 1 Ω-cm. The native oxide was first removed by HF. Next, the wafer surface was etched using a 25% KOH solution at 60 °C for 30 min to remove any possible saw damage. Afterwards, the wafers were cleaned via a standard cleaning procedure [13–15] to remove any organic and ion contaminants.

2.2. 532 nm wavelength laser processing

As shown in Fig. 1a, a single-pulse-processing technique was applied to the 532 nm laser processed samples. The unique single-laser-processed-spot design allowed the study of phase changes along the spatial profile under a Gaussian beam. Also, use of a single shot avoids additional influence from multiple pulses. Through setting the pulse repetition rate at 30 kHz and scanning speed at 300 mm/s, we achieve adjacent melt spots as shown in the scanning electron microscope (SEM) image in Fig. 1b.

The 532 nm wavelength laser used was a pulsed ytterbium fiber laser (model YLP-G-10, IPG Photonics) with a full laser power of 10 W at the 100% set point and a laser pulse width of 1.3 ns. The laser beam entered a galvanometer scanner (SCANcube 14, Scanlab) and was scanned onto the silicon sample with a beam size focused to 25 μm (schematic shown in Reference [13,14]).

The laser processing fluences were varied. Most laser-based silicon solar cell processing requires silicon melting or ablation. For example, the silicon melting is required in the laser doping process to allow the dopants to diffuse into the silicon [8–10], and the silicon ablation is required in the laser microtexturing [4,5] and laser edge isolation [6,7]. In order to relate our study to Si solar cells processing, the laser fluences were chosen at 1.31 J/cm^2 and 1.64 J/cm^2, near and above the melt threshold. At 1.31 J/cm^2 fluence, the processed spot can be observed under the TEM with a spot size of ~2 μm. At 1.64 J/cm^2 fluence, the melted spot size became 10.64 μm as shown in the SEM image (Fig. 1b).

2.3. 1064 nm wavelength laser processing

A 1064 nm wavelength pulsed fiber laser was used to process silicon wafers. The full laser power was 30 W at a 100% set point and the pulse duration was 50 ns. For 1064 nm laser processed samples, the entire sample area was processed. The repetition rate was set at 30 kHz, the scanning speed was 50 mm/s, and the line spacing was 20 μm, which guaranteed uniform laser-treated regions.

The laser fluences were varied at different levels, namely, 1.28 J/cm^2, 1.47 J/cm^2, and 1.60 J/cm^2. Visible melting started at 1.28 J/cm^2 fluence, while the surface morphology changes became significant at 1.60 J/cm^2 (SEM images in Reference [13]).

2.4. Phase transformation characterization

The phase transformation was investigated through TEM and Raman spectroscopy. By imaging the cross-section of a laser processed spot under TEM, phase changes and their locations can be determined in diffraction mode. Additionally, Raman spectroscopy with an analysis spot size of around 1 μm (Fig. 1a) was used for line-mapping across the laser processed spot to confirm Si phases at different positions.

2.4.1. Transmission electron microscopy (TEM)

For detailed microstructure observation, cross-sectional TEM images were taken by a JEOL 2000FX at an incident electron beam energy of 200 keV equipped with a slow-scan and wide-angle TV-rate camera (Gatan, Inc.). The spatial resolution was 0.3 nm.

To prepare cross-sectional TEM samples, laser processed silicon wafers were first cut into 2 mm × 1 mm pieces. After a suitable amount of epoxy glue was spread uniformly on the surface, two pieces were glued face-to-face. The adjoined sample was vertically (1 mm direction) glued onto a supportive Cu grid with a small amount of epoxy. The grid was then glued with thermo-wax on top of a glass cylinder. With help of the glass cylinder, the sample was manually polished down to around 50 μm via sandpaper (800 grit and 2000 grit). The thickness was monitored via a Zygo white-light interferometer. Next, the sample was ion-milled to 10–50 nm using a GATAN 691 Precision Ion Polishing System (PIPS).

2.4.2. Raman spectroscopy

Raman spectra were taken on Renishaw inVia Raman Microscope. A 405 nm wavelength laser was used for excitation in the surface region for the sample. The power percentage was set at 0.05% to achieve a small analysis size of 1 μm. The comparative size of the Raman laser spot is shown in Fig. 1a. The laser beam moved across the processed spot with 1 μm steps to acquire the line-scan. Due to the small spatial

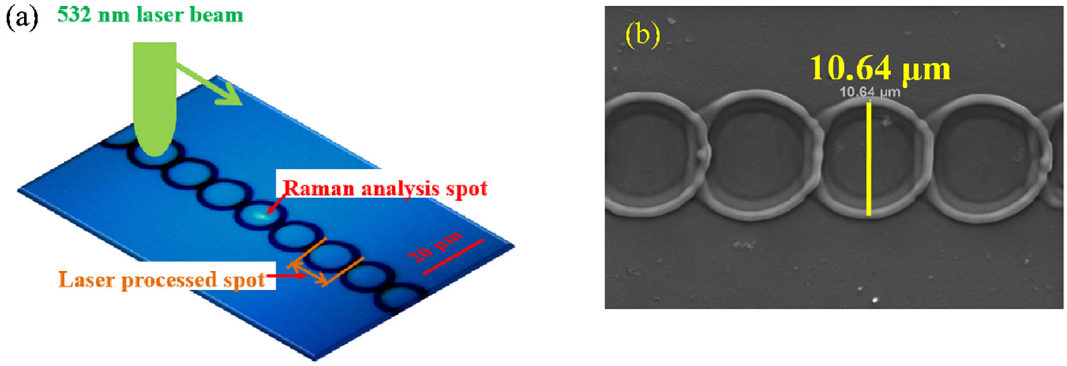

Fig. 1. (a) Schematic showing single-pulse laser processed silicon and local characterization of phase transformation using cross-section TEM and Raman line-mapping. (b) SEM image showing adjacent processed spots created via laser fluence of 1.64 J/cm^2 and wavelength of 532 nm.